JGR Space Physics

RESEARCH ARTICLE
10.1029/2019JA027501

Plasma Depletion Bays in the Equatorial Ionosphere Observed by FORMOSAT-3/COSMIC During 2007–2014

F. Y. Chang[1], J. Y. Liu[1,2,3], T. W. Fang[4,5], P. K. Rajesh[6], and C. H. Lin[6]

[1]Center for Astronautical Physics and Engineering, National Central University, Taoyuan, Taiwan, [2]Institute of Space Science, National Central University, Taoyuan, Taiwan, [3]Center for Space and Remote Sensing Research, National Central University, Taoyuan, Taiwan, [4]Cooperative Institute for Research in Environmental Sciences, University of Colorado Boulder, Boulder, CO, USA, [5]Space Weather Prediction Center, National Oceanic and Atmospheric Administration, Boulder, CO, USA, [6]Department of Earth Sciences, National Cheng Kung University, Tainan, Taiwan

Key Points:
- A new feature of plasma depletion bays (PDBs) in the electron density fixedly appears over the equatorial/low-latitude nighttime ionosphere
- PDBs prominently appear in particular longitudes, summer hemisphere, nighttime, solstice months, and low solar activity years
- Horizontal wind model simulations show that the zonal neutral winds projected on the magnetic field lines are essential to form PDBs

Correspondence to:
J. Y. Liu,
jyliu@jupiter.ss.ncu.edu.tw

Citation:
Chang, F. Y., Liu, J. Y., Fang, T. W., Rajesh, P. K., & Lin, C. H. (2020). Plasma depletion bays in the equatorial ionosphere observed by FORMOSAT-3/COSMIC during 2007–2014. *Journal of Geophysical Research: Space Physics*, *125*, e2019JA027501. https://doi.org/10.1029/2019JA027501

Received 5 OCT 2019
Accepted 5 AUG 2020
Accepted article online 22 AUG 2020

Abstract A new feature of plasma depletion bay (PDB) on the longitudinal structure over the equatorial and low latitudes is observed by the FORMOSAT-3/COSMIC (F3/C) electron density profiles. The existence of the PDB feature is confirmed by the OI 135.6 nm radiance from TIMED/GUVI, which together with F3/C electron density shows that one North PDB extending to the Southern Hemisphere prominently appears over Southwest America while three South PDBs extending to the Northern Hemisphere occur over North Atlantic, India Ocean, and Southeast Asia. Three-dimensional F3/C ionospheric electron densities are further used to examine PDB structures at various local times, seasons, solar activities, and altitudes during 2007–2014. It is found that the north PDB is observed during October–March, while the south PDBs mostly exist during April–September. These PDBs can be observed within 250–350 km altitudes in the nighttime, appearing pronounced over 275–300 km altitudes around 2300–0100 LT, in the low solar activity year of 2007. Global effective wind patterns computed using the horizontal wind model HWM93 in solstice months suggest that summer-to-winter field-aligned winds projected from zonal neutral winds play an important role.

1. Introduction

An enormous amount of energy has been constantly irradiating from the Sun and into space in the forms of electromagnetic waves and solar winds. The energy radiated by these electromagnetic waves determines the structures and dynamics of the atmosphere and the ionosphere. Consequently, the low-latitude ionosphere exhibits a highly dynamic environment with variations of local time, season, solar cycle, altitude, geographic location, etc. To globally observe ionospheric weather resulting from these variations, satellites measurements are ideally employed. For example, nightglow images of OI 135.6 nm from the far ultraviolet emission observation on board the NASA Imager for Magnetopause-to-Aurora Global Exploration (IMAGE) and the Global Ultraviolet Imager (GUVI) on board the Thermosphere Ionosphere Mesosphere Energetics and Dynamics (TIMED) satellites have been used to study the longitudinal structure of the equatorial anomaly in the nighttime ionosphere (Immel et al., 2006; Kil et al., 2015; Sagawa et al., 2005). Meanwhile, the GPS occultation experiment (GOX) on board the FORMOSAT-3/COSMIC (F3/C) mission, which consists of six microsatellites, has proven to be a powerful tool in sounding vertical profiles of the ionospheric electron density by its global-coverage observations. By accumulating radio occultation (RO) observations, unprecedented detail of the three-dimensional ionospheric electron density structure can be constructed (Lin et al., 2007, 2010).

In this study, the potential of space-based observations in identifying global electron density variations has been further utilized to investigate a new kind of ionospheric feature, named as plasma depletion bay (PDB). As the name indicates, PDB is a broad region of low-density plasma at low-latitude, giving a visual appearance of low plasma density in winter hemisphere extending to the summer hemisphere of generally high plasma density, which we call plasma depletion bay or PDB, as it appears like ocean water finding its way to low-level lands forming ocean bays. The black and red circled regions in Figure 1 illustrates PDBs observed simultaneously in F3/C electron density and TIMED/GUVI OI 135.6 nm intensity around 2100

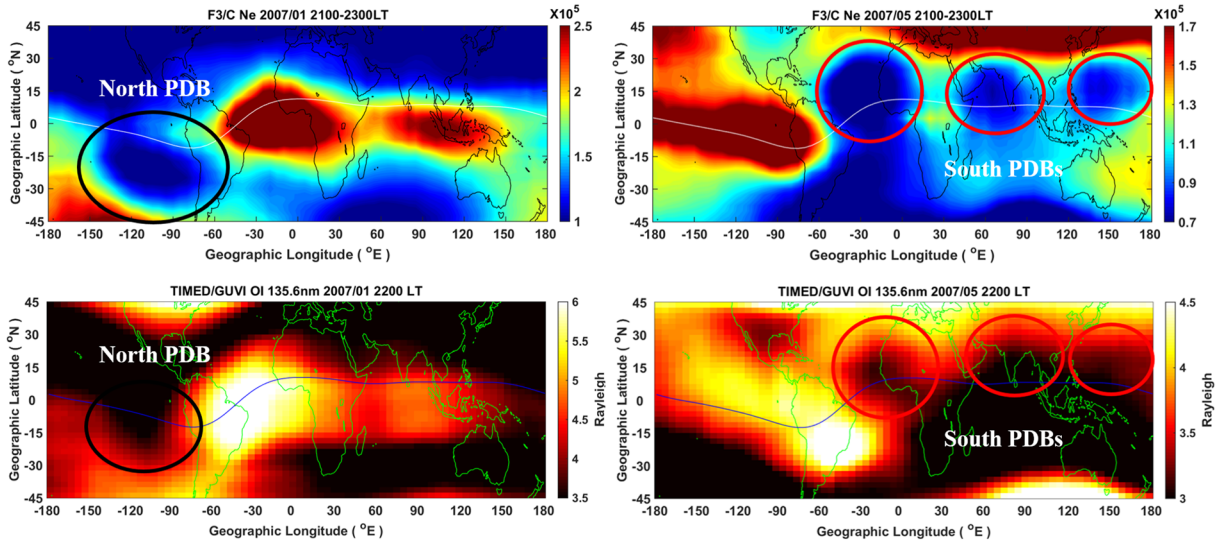

Figure 1. The F3/C electron density as well as TIMED/GUVI OI 135.6 nm intensity at 275 km altitude at 2100–2300 LT in January (left two panels) and May (right two panels) 2007. Black and red circles denote the one North PDB and three South PDBs. The spatial resolution in longitude and latitude are 5° and 2.5°.

LT, in the months of January and May of 2007. It is remarkable to note that both the F3/C electron density and TIMED/GUVI airglow intensity weaken with a slightly southward curving to the Southern Hemisphere (i.e., opening to the Northern Hemisphere; north plasma depletion bay, North PDB) over Southwest America longitude of 75–135°W in January 2007, while similar features but with three slightly northward curving to the Northern Hemisphere (i.e., opening to the Southern Hemisphere; South PDBs) could be seen over North Atlantic (60°W to 30°E), India Ocean (45–110°E), and Southeast Asia (120–170°E) longitudes in May 2007. The agreement in the independent observations by both F3/C and TIMED/GUVI observations strongly suggests that PDB is a nighttime electron density depletion feature produced by ionospheric variations, irrespective of measurement techniques or inversion algorithms.

In addition to reporting the new feature of PDBs, this study examines the associated diurnal, seasonal, solar activity, and vertical variations by taking advantage of the three-dimensional F3/C RO electron density profiles during the years 2007–2014. Furthermore, meridional and zonal neutral winds obtained from Horizontal Wind Model 1993, HWM93, (Hedin et al., 1996) are used to discuss and understand the possible physical mechanisms.

2. Observation

The F3/C occultation observations are first subdivided into 12 months by binning about 60 days of data (i.e., from 15 days prior till 15 days after for each month) in every 2-hr interval and taking median value of the soundings within each 5°-by-2.5° (longitude-by-latitude) grid at 25 km altitude levels. Figure 2 displays monthly variations of the electron density at 275 km altitude at 2300 LT in 2007. The single North PDB appears during October–March, while the three South PDBs occur during April–September. The North PDB appear prominent in December (summer solstice in the Southern Hemisphere), whereas the South PDBs become prominent in June (summer solstice in Northern Hemisphere). Figure 3 shows the electron density at 275 km altitude at various fixed local time from 0700 to 0500 LT in December and June of 2007. It can be seen that the North PDB and the South PDBs start developing around 2100 LT, become prominent during 2300–0100 LT, diminishes after 0300 LT, and are indiscernible after 0500 LT.

Figure 4 shows the solar activity variation of the PDB features at 275 km altitude, at 2300 LT, in the months of December and June during 2007–2014. The *F*10.7 index (the solar radio flux at 10.7 cm) in the low solar activity years of 2007–2010 and the high solar activity years of 2011–2014 average at about 75 (65–85) and 130 (100–160) sfu (solar flux unit), respectively. It can be seen that the PDBs yield more prominent structures during the low solar activity than in high solar activity years. Figure 5 illustrates the electron density over 250–550 km altitudes in December and June in 2007. Both the North PDB and South PDBs can be clearly

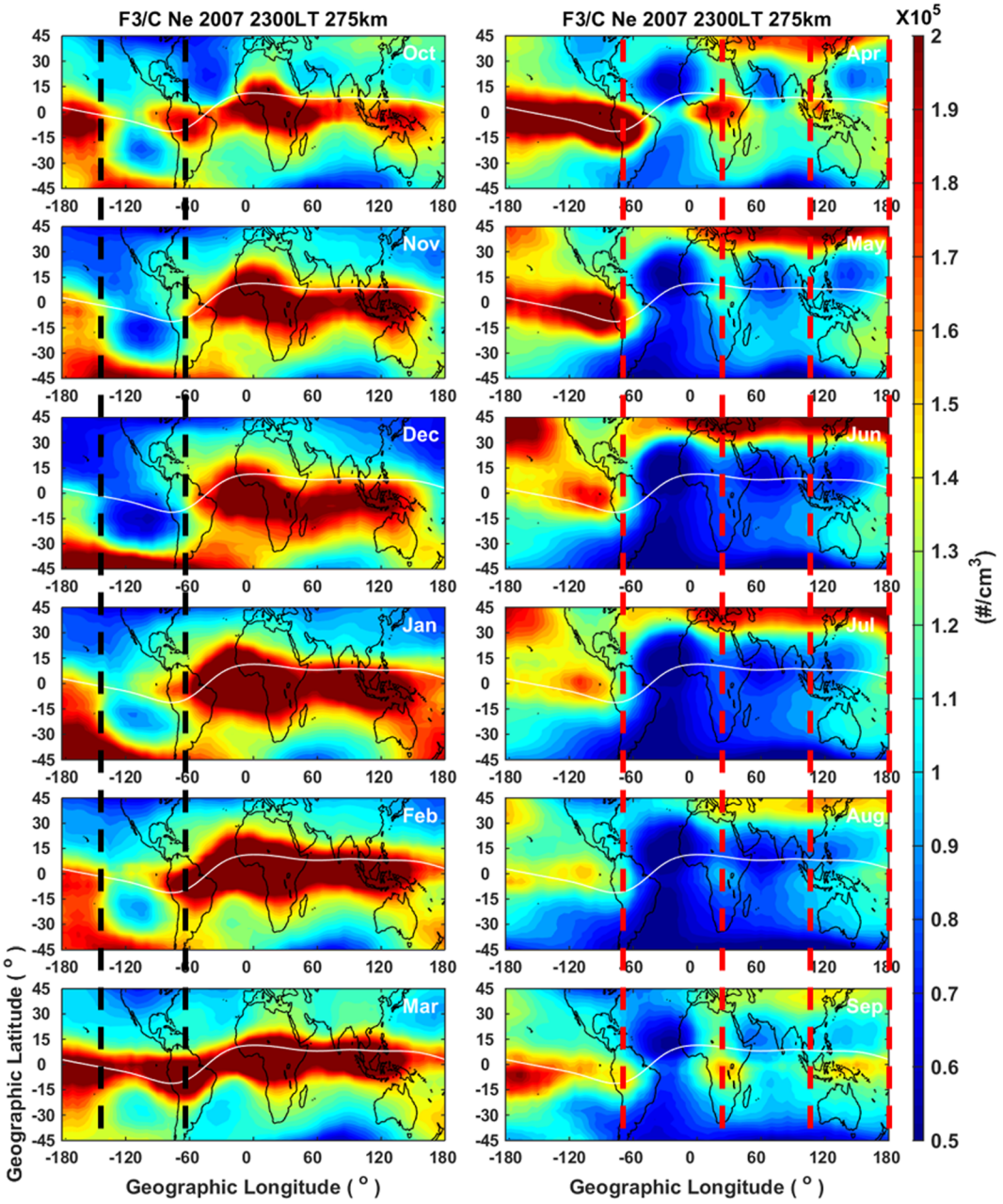

Figure 2. Monthly plots of the electron density at 275 km in the global constant local time maps at 2300 LT of 2007. Black and red dash lines indicate the longitudinal sectors of the one North PDB and the three South PDBs, respectively.

observed in height range of 250–350 km altitudes. The most prominent features of both the North and South PDBs are visible at 275 km altitude. From the figure, it is worth to note that when the altitude increases, the curving of the North PDB and the South PDBs shift northward and southward, respectively (i.e., equatorward).

3. Discussion and Conclusion

Both F3/C electron density and TIMED/GUVI OI 135.6 nm intensity simultaneously observe the one North PDB and three South PDBs (Figure 1), independently confirming the existence of the plasma depletion bay. Recently, there has been several studies reporting longitudinal Wave Number 4 variations of nonmigrating

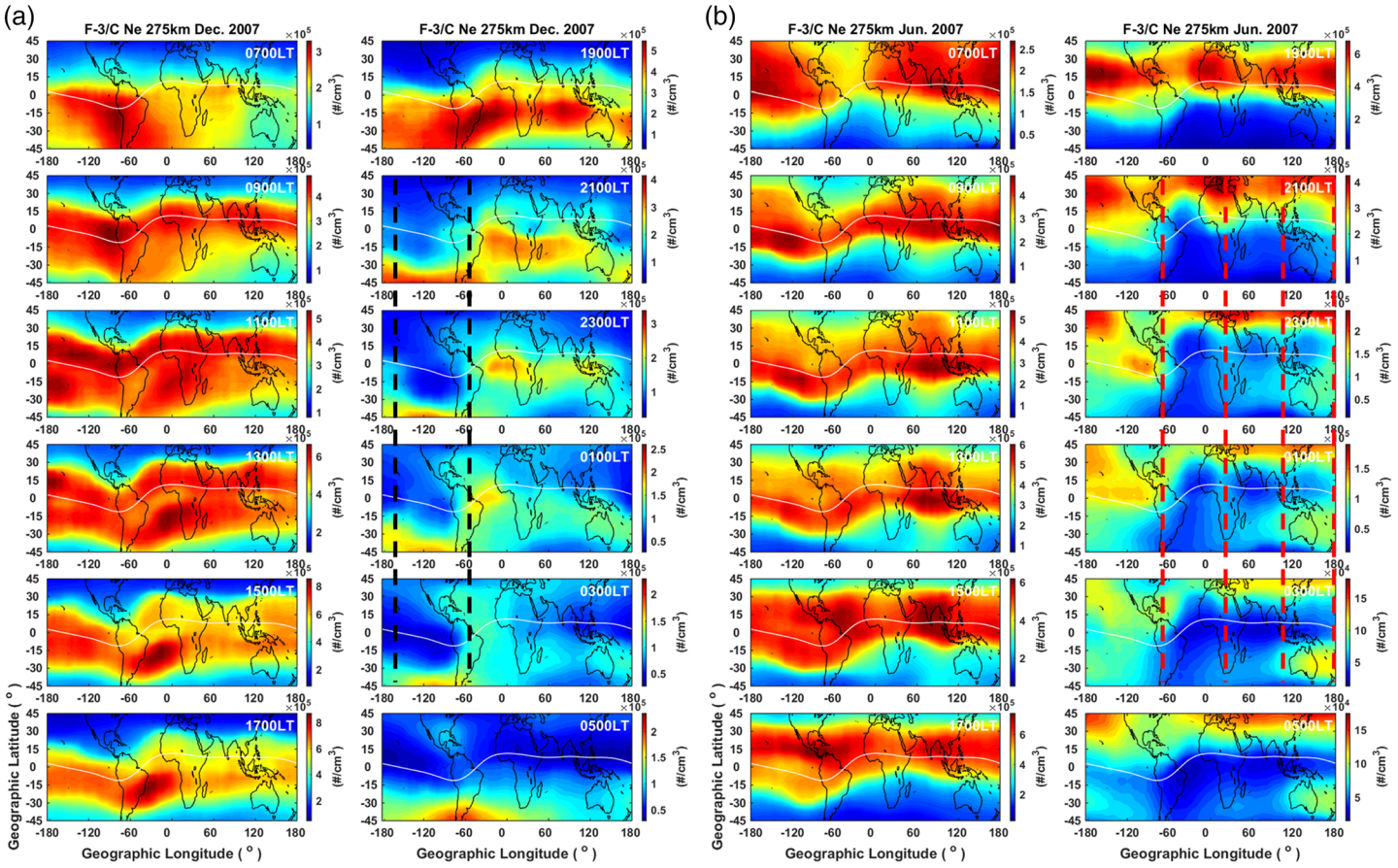

Figure 3. Temporal variations of the PDB longitudinal structures of F3/C electron density at 275 km at various global fixed local time in (a) December solstice and (b) June solstice 2007.

tides in the equatorial ionosphere (Immel et al., 2006; Kil et al., 2015; Lin et al., 2007; Sagawa et al., 2005). It is necessary to distinguish PDBs from such Wave 4 modulations. Note that Wave 4 patterns are pronounced during daytime, especially around local noon and prominently occurs during equinox months (Ren et al., 2008). Wan et al. (2008) report that the Wave 4 patterns become prominent during high solar activities. On the contrary, the PDB features occur near local midnight and is pronounced in solstice months with low solar activity conditions.

It can be further seen that the North PDB and the South PDBs at the equatorial/low-latitude regions are almost stationary at various local times (Figure 3), while the four-peaked pattern of nonmigrating tides yield eastward shifts (Immel et al., 2006; Lin et al., 2007; Sagawa et al., 2005; Wan et al., 2008). Lin et al. (2007) used integrated electron content between 400 and 450 km, sounded by using F3/C, to study the nonmigrating tide (i.e., Wave Number 4) at various local time over the equatorial region. They found four-peaked structures with eastward motions of 42–88 m/s, being most prominent at daytime during 1200–1600 LT, become less prominent during 1600–2000 LT, and eventually become discernible during 2000–2200 LT. These discrepancies in the local time (night/day), season (solstice/equinox), and solar activity (low/high) of prominent occurrence of PDB/Wave 4 pattern, as well as the appearance without/with eastward motions, show that the PDB and the Wave Number 4 are two different features with different physical mechanism, and further confirm that PDB's are new phenomena revealed by the 3-D space-based soundings by F3/C.

After having established the existence of PDBs, we further investigate the possible physical and dynamical processes that give rise to such variations. Figure 4 reveals that the PDBs prominently appear in the low solar activity period in 2007–2010, which might be because of the ionospheric plasma density being low during this period due to less intense solar radiation. With less background density, the relative variations

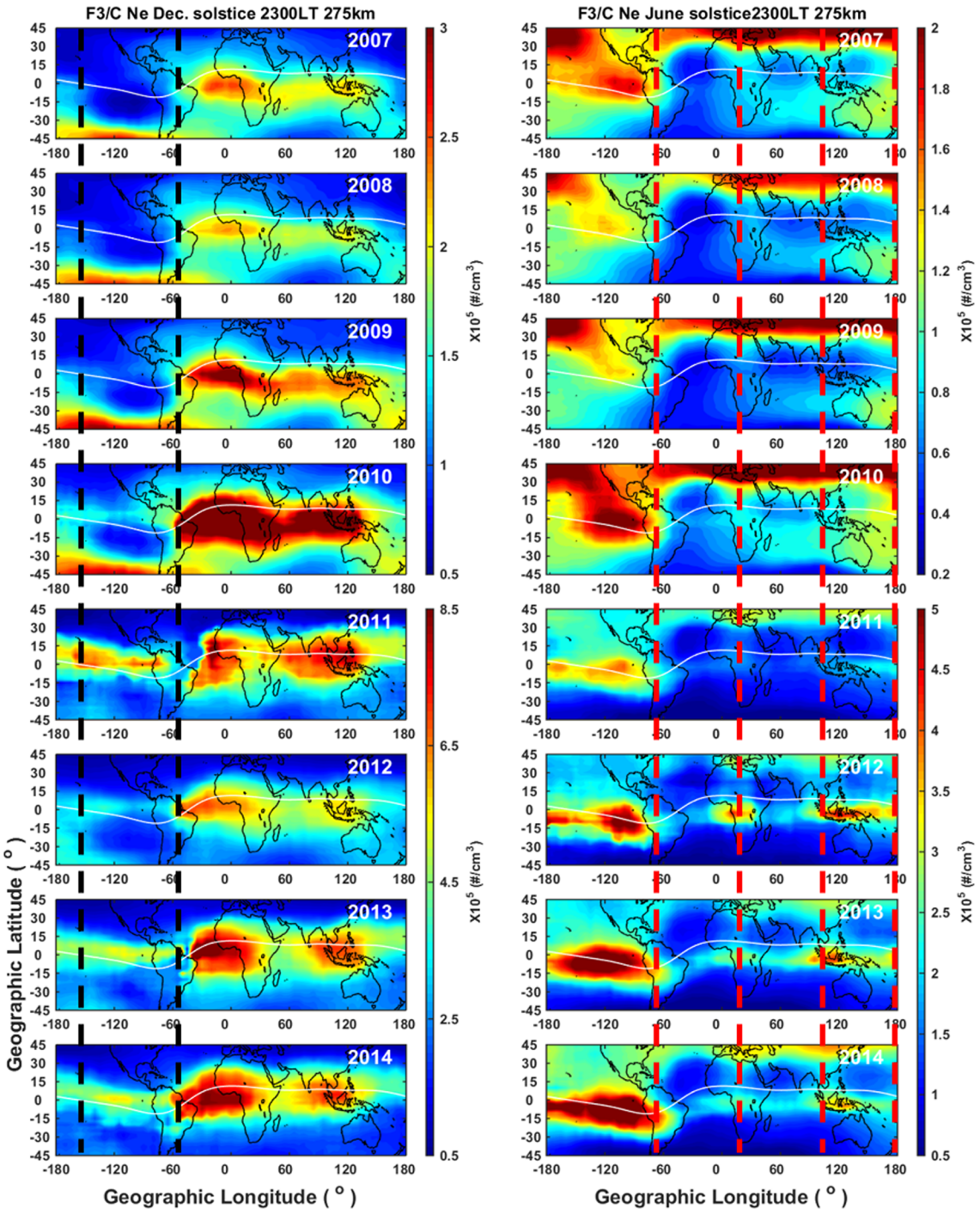

Figure 4. Yearly plots of the electron density at 275 km in the global constant local time maps at 2300 LT during December solstice (left panels) and June solstice (right panels) of 2007–2014.

become more pronounced. Besides the solar radiation effect, observations and simulations (Fesen et al., 2000) show that in the postsunset equatorial ionosphere, the upward $E \times B$ drift of the prereversal enhancement (PRE) is greater in high solar activities than low solar activities. This results in the nighttime plasma being pumped into higher and lower altitudes during high and low solar activities, respectively (cf. Fejer et al., 1991). Since the molecular collision is inversely proportional to altitude, a relatively weak upward $E \times B$ drift of the PRE transports plasma into a relatively low altitude in the

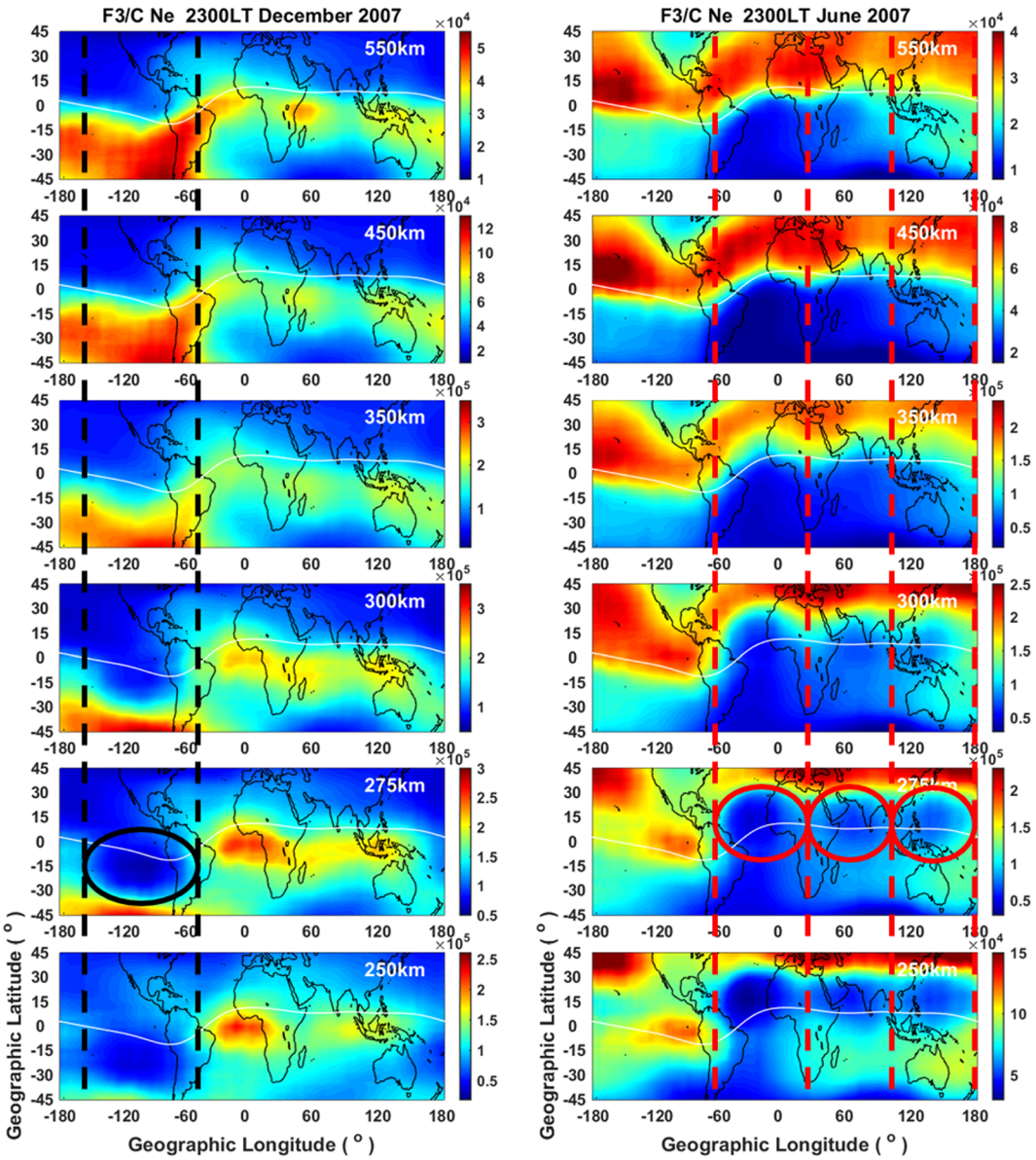

Figure 5. Altitudinal plots 250–550 km altitudes in the global constant local time maps at 2300 LT during December solstice (left panels) and June solstice (right panels) of 2007. The one North PDB and three South PDBs appear prominently at 275 km altitude denoted by black and red circles.

ionosphere, where the loss process rate is larger and results in the plasma density being less during low solar activities.

The plasma density depletion over PDBs could be caused by much faster chemical recombination (or loss), which could result in an overall decrease of plasma density at lower altitudes in nighttime periods of 19 to 03 LT. However, the plasma density over the PDB regions is much lower than that over neighboring longitudes, where also such faster chemical recombination should occur around low latitudes. This suggest that in addition to the overall recombination loss, there would be additional physical mechanisms for the peculiar feature of PDB. Meanwhile, the seasonal characteristic in the occurrence of PDBs (Figure 2), with the North PDB prominently appearing in the Southern Hemisphere in December (southern summer), and the South PDBs occurring pronounced in the Northern Hemisphere in June (northern summer) indicates that summer-to-winter neutral wind might be essential in producing these features. With weaker PRE as discussed above, dynamic variations such as those by summer-to-winter neutral wind would be more

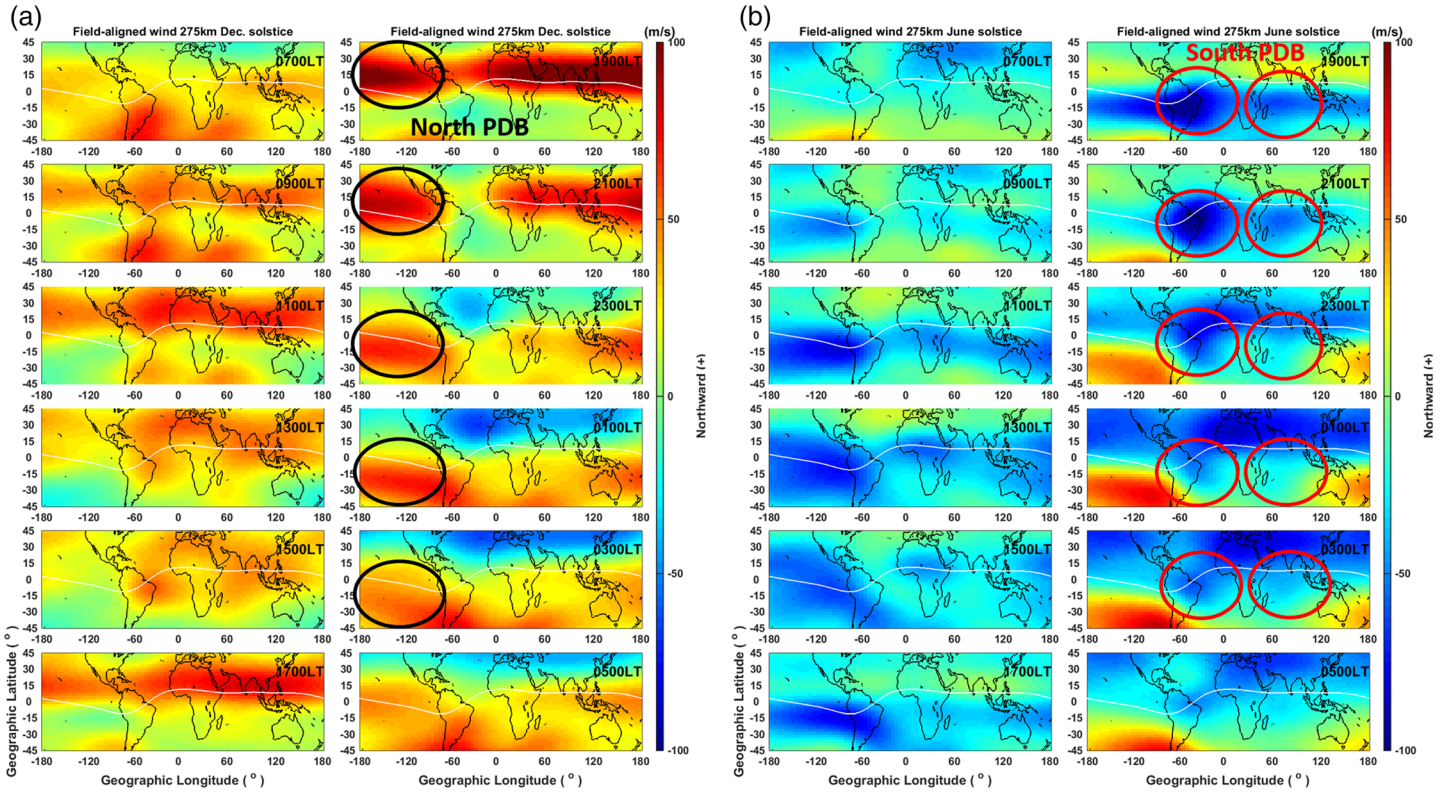

Figure 6. Field-aligned winds U combined by HWM93 zonal neutral winds V_x and meridional neutral winds V_y at 275 km at various global fixed local time during (a) December solstice and (b) June solstice. Positive wind values indicate northward flow. Black and red circles indicate corresponding regions of the one North PDB and three South PDBs in electron density maps (e.g., Figure 3).

effective in redistributing plasma along field lines and changing the overall recombination loss, which seems to result in the plasma depletion bays in low solar activity periods. In the solstice, the summer-to-winter wind affects the global circulation and thereby creates the thermosphere spoon effect to reduce the global $[O]/[N_2]$ and leads to overall smaller electron density during solstice (Fuller-Rowell, 1998). The summer-to-winter wind also leads to an upwelling in the summer hemisphere and a downwelling in the winter hemisphere and thus the $[O]/[N_2]$ tends to decrease in the summer but increase in the winter. Although the summer-to-winter wind produces asymmetric $[O]/[N_2]$ responses, the overall $[O]/[N_2]$ effect is smaller in solstices compared to equinoxes, which contributes to the semiannual variation of the ionosphere. The plasma transported from summer to winter hemisphere is pushed to lower altitude and should encounter more molecular nitrogen and loss.

To further examine the neutral wind effect in the PDB formation, we compute the transequatorial field-aligned winds from HWM93. Several studies (Chang et al., 2015; Liu et al., 2014; Titheridge, 1995) have reported that the topside ionospheric plasma density and the thermospheric neutral winds undergo a strong longitudinal effect, with the actual nature of effect depending on the configuration of the magnetic field. Thus, to investigate the effect of neutral wind in modifying plasma density, the parallel component of neutral wind (parallel to the magnetic field lines) are computed. Let V_x and V_y be the geographical zonal (eastward positive) and meridional (equatorward positive) wind components derived by HWM93, and D and I be the magnetic declination and inclination angles obtained from International Geomagnetic Reference Field (IGRF-12), respectively. Hence, the field-aligned wind U derived from the meridional and zonal neutral wind in magnetic meridional direction can be expressed as

$$U = V_x \sin D \cos I + V_y \cos D \cos I \tag{1}$$

Figure 6 is the field-aligned wind U contributed from V_x and V_y components at 275 km altitude in December solstice and June solstice. Here positive values represent northward wind and negative

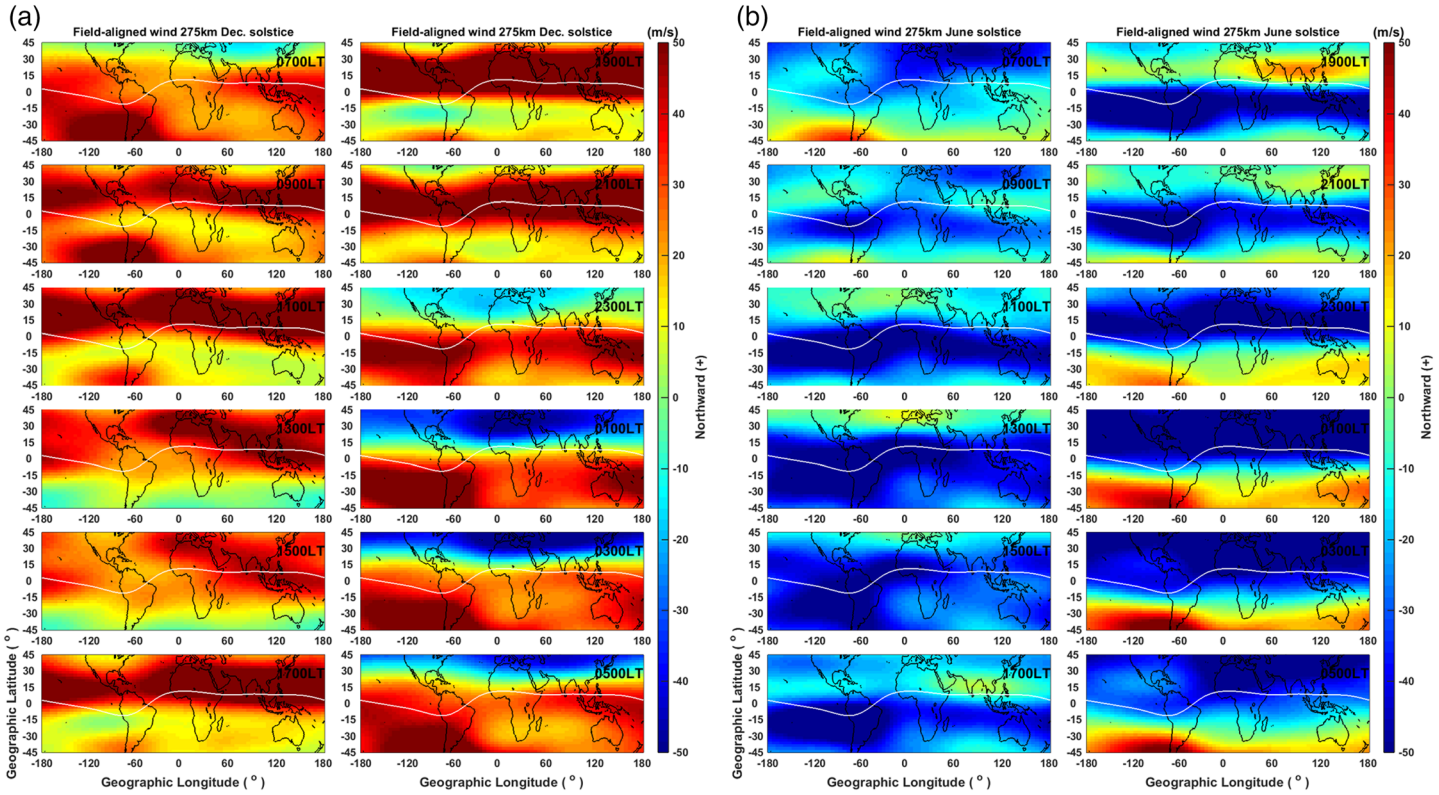

Figure 7. Field-aligned winds U_m contributed by meridional neutral winds V_y at 275 km at various global fixed local time during (a) December solstice and (b) June solstice. Positive wind values indicate northward flow.

indicate southward wind. The result shows that field-aligned wind U over the region of the North PDB in December solstice (Figure 3a) tends to blow from the Southern Hemisphere to the Northern Hemisphere (summer-to-winter wind). Similarly, over the regions of the South PDBs (Figure 3b), two groups of summer-to-winter wind from the Northern Hemisphere to the Southern Hemisphere overlap with two of the three South PDBs (North Atlantic region around 0–60°W and India Ocean region around 45–110°E).

To further understand the contribution in the two components of meridional wind and zonal wind over regions of PDBs, Figures 7 and 8 individually examine the field-aligned wind U_m and U_z calculated by the second and first terms of Equation 1, by using meridional and zonal neutral wind components separately. Figure 7 shows that the field-aligned summer-to-winter wind U_m computed by the meridional neutral wind blows from the summer hemisphere to the winter hemisphere (southern summer in December solstice and northern summer in June solstice). The result generally displays a continuous pattern in the ionosphere without significant longitudinal variations in the equatorial and low latitudes, while the characteristics of the observed PDBs could not be fully explained by the field-aligned winds driven from meridional neutral winds. It can be seen from Figure 8 that a prominent field-aligned summer-to-winter wind U_z from the zonal neutral wind appears coincidently with the North PDB during nighttime of 1900–0100 LT of December, while two groups of field-aligned summer-to-winter winds U_z overlap with the three South PDBs during the nighttime of 1900–0300 LT of June (Figures 1–5). These coincidences provide evidence to support that the summer-to-winter winds mostly given by zonal neutral winds (Figure 8) are thought to contribute to the ionospheric plasma density variations over the PDBs longitude sectors in the nighttime as described in this study (Figures 1–5).

Figures 6 and 8 agree with the previous studies that large neutral zonal winds play a predominant role in the variation of F region parameters at low latitudes by uplifting or lowering the plasma density along the magnetic field lines (Kil et al., 2006; Venkatraman & Heelis, 2000). West and Heelis (1996) reported that the summer-to-winter meridional winds play a dominant role at low latitudes in regulating the F peak height,

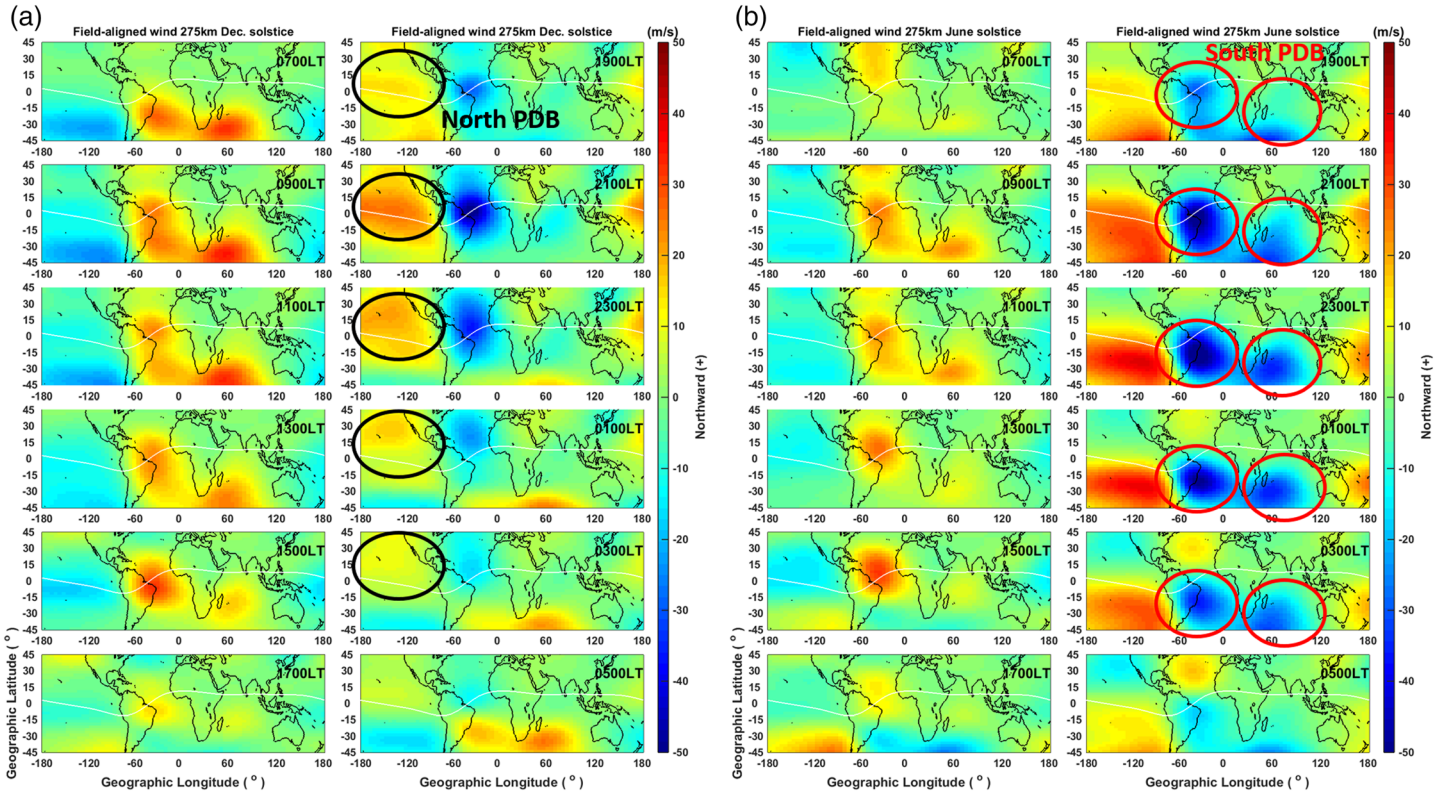

Figure 8. Field-aligned winds U_z contributed by zonal neutral winds V_x at 275 km at various global fixed local time during (a) December solstice and (b) June solstice. Positive wind values indicate northward flow. Black and red circles indicate regions of the one North PDB and three South PDBs.

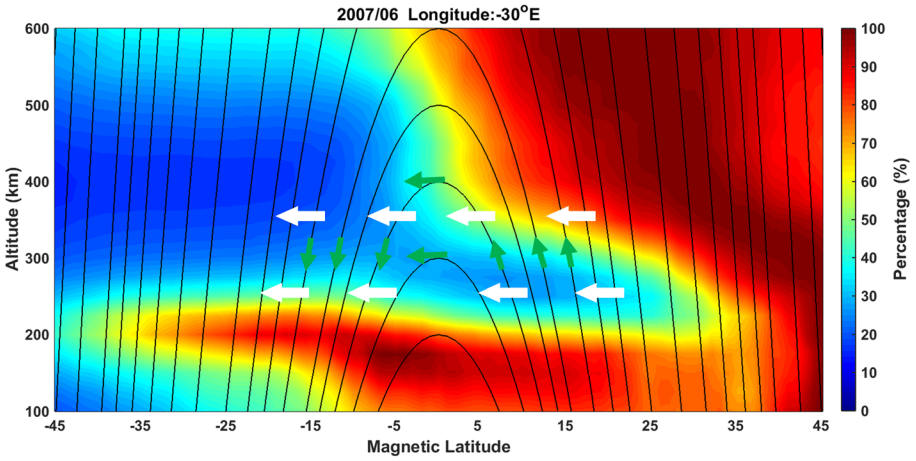

Figure 9. A schematic diagram of summer-to-winter winds (white arrows) on the PDB longirudinal sector. The background electron density is the altitude-latitude cut along the −30°E longitude extracted from Figure 5 and is normalized at each altitude. In the summer hemisphere, the summer-to-winter wind will produce parallel plasma drift (green arrows), moving plasma upward and equatorward to higher altitudes in the summer hemisphere. In the winter hemisphere, the summer-to-winter winds are poleward, moves plasma down along the field lines in the winter hemisphere to lower altitudes, where they are lost due to recombination, results in the plasma density decrease overall in the winter hemisphere ionosphere.

with the zonal neutral winds enhancing or opposing the effects of the field-aligned winds at longitudes with significant magnetic declination under solstice conditions. The dynamic interactions discussed above, resulting in the generation of PDB are summarized using the sketch in Figure 9. For summer-to-winter winds, equatorward winds drag the plasma along the magnetic field lines upward to higher altitude and forms the PDB at lower altitude in the summer hemisphere. Poleward winds in the winter hemisphere accelerate the downward plasma diffusion, which cause an overall decrease of plasma density at lower altitudes where recombination is faster. Thus, summer-to-winter winds drag the plasma along the magnetic field line (or flux tube), ascending from the low-latitude ionosphere in the summer hemisphere, horizontally across the magnetic equator, and descending to the low-latitude ionosphere in the winter hemisphere. The less dense plasma density at the low-latitude ionosphere in the summer hemisphere will be dragged upward/equatorward, which results in the PDB curving feature to move equatorward with altittude in the summer hemisphere (Figure 5). As the wind blows to the winter hemisphere over the magnetic equator, the plasma is transported downwand/poleward along the same magnetic field line from higher to lower altitudes. With the recombination loss processes being inversely propontional to the altitude, plasma density drastically decreases at the low-altitude off-equator ionosphere in the winter hemisphere.

Note that both F3/C and TIMED/GUVI simultaneously observed the third South PDB over the Southeast Asia sector (135–165°E), while HWM93 failed to simulate and reproduce it. Note that HWM is an empirical model, which is constructed by using various kinds of observations, such as winds inferred from satellite probing and radar sounding on plasma, airglow, etc. Thus, lack of sufficient observations over this longitude region might be impacting the model prediction. The discrepancy of the third PDB in the Southeast Asia sector suggests that the F3/C electron density observations might in turn benefit to fine tune the HWM development in the future.

This paper for the first time reports the nighttime plasma depletion bay in the equatorial and low-latitude ionosphere, with a stationary North PDB appearing over Southwest America during October–March, and three South PDBs located occur over North Atlantic, Indian Ocean, and Southeast Asia during April–September. The PDBs prominently appear during nighttime, in solstice seasons, and low solar activity periods. In conclusion, the relative and net effect of the three processes that the summer-to-winter wind (1) causes summer-to-winter plasma flow, (2) raises the ionosphere in height in the summer hemisphere, and (3) reduces the $[O]/[N_2]$ in summer hemisphere, are significant for the PDB formation.

Data Availability Statement

The TIMED/GUVI data for this paper are available at this website (http://guvitimed.jhuapl.edu/home_background).

Acknowledgments

The authors gratefully acknowledge the Taiwan Analysis Center for COSMIC (TACC) and COSMIC Data Analysis and Archive Center (CDAAC) for providing FORMOSAT-3/COSMIC data (https://tacc.cwb.gov.tw/, http://cdaac-www.cosmic.ucar.edu/). This work was financially supported by the Center for Astronautical Physics and Engineering (CAPE) from the Featured Area Research Center program within the framework of Higher Education Sprout Project by the Ministry of Education (MOE) in Taiwan. This study is supported by the Ministry of Science and Technology (MOST) Grant MOST 106-2628-M-008-002 in Taiwan and the ISSI-Bern International Team of "Ionospheric Space Weather Studied by RO and Ground-based GNSS TEC Observations" (the team leader Liu, J. Y. Tiger [TW]).

References

Chang, F. Y., Liu, J. Y., Chang, L. C., Lin, C. H., & Chen, C. H. (2015). Three-dimensional electron density along the WSA and MSNA latitudes probed by FORMOSAT-3/COSMIC. *Earth, Planets and Space*, *67*, 156. https://doi.org/10.1186/s40623-015-0326-8

Fejer, B. G., de Paula, E. R., González, S. A., & Woodman, R. F. (1991). Average vertical and zonal *F*-region plasma drifts over Jicamarca. *Journal of Geophysical Research*, *96*(A8), 13,901–13,906. https://doi.org/10.1029/91JA01171

Fesen, C. G., Crowley, G., Roble, R. G., Richmond, A. D., & Fejer, B. G. (2000). Simulation of the pre-reversal enhancement in the low latitude vertical ion drifts. *Geophysical Research Letters*, *27*(13), 1851–1854. https://doi.org/10.1029/2000GL000061

Fuller-Rowell, T. J. (1998). The "thermospheric spoon": A mechanism for the semiannual density variation. *Journal of Geophysical Research*, *96*(A8), 13,901–13,906. https://doi.org/10.1029/91JA01171

Hedin, A. E., Fleming, E. L., Manson, A. H., Schmidlin, F. J., Avery, S. K., Clark, R. R., et al. (1996). Empirical wind model for the upper, middle and lower atmosphere. *Journal of Atmospheric and Terrestrial Physics*, *58*(13), 1421–1447. https://doi.org/10.1016/0021-9169(95)00122-0

Immel, T. J., Sagawa, E., England, S. L., Henderson, S. B., Hagan, M. E., Mende, S. B., et al. (2006). Control of equatorial ionospheric morphology by atmospheric tides. *Geophysical Research Letters*, *33*, L15108. https://doi.org/10.1029/2006GL026161

Kil, H., DeMajistre, R., Paxton, L. J., & Zhang, Y. L. (2006). Nighttime *F*-region morphology in the low and middle latitudes seen from DMSP F15 and TIMED/GUVI. *Journal of Atmospheric and Solar-Terrestrial Physics*, *68*(14), 1672–1681. https://doi.org/10.1016/j.jastp.2006.05.024

Kil, H., Kwak, Y.-S., Lee, W. K., Krall, J., Huba, J. D., & Oh, S. -J. (2015). Nonmigrating tidal signature in the distributions of equatorial plasma bubbles and prereversal enhancement. *Journal of Geophysical Research: Space Physics*, *120*, 3254–3262. https://doi.org/10.1002/2014JA020908

Lin, C. H., Hsiao, C. C., Liu, J. Y., & Liu, C. H. (2007). Longitudinal structure of the equatorial ionosphere: Time evolution of the four-peaked EIA structure. *Journal of Geophysical Research*, *112*, A12305. https://doi.org/10.1029/2007JA012455

Liu, J. Y., Chang, F. Y., Oyama, K. I., Kakinami, Y., Yeh, H. C., Yeh, T. L., et al. (2014). Topside ionospheric electron temperature and density along the Weddell Sea latitude. *Journal of Geophysical Research: Space Physics*, *120*, 609–614. https://doi.org/10.1002/2014JA020227

Liu, J. Y., Lin, C. Y., Lin, C. H., Tsai, H. F., Solomon, S. C., Sun, Y. Y., et al. (2010). Artificial plasma cave in the low-latitude ionosphere results from the radio occultation inversion of the FORMOSAT-3/COSMIC. *Journal of Geophysical Research*, *115*, A07319. https://doi.org/10.1029/2009JA015079

Ren, Z., Wan, W., Liu, L., Zhao, B., Wei, Y., Yue, X., & Heelis, R. A. (2008). Longitudinal variations of electron temperature and total ion density in the sunset equatorial topside ionosphere. *Geophysical Research Letters*, *35*, L05108. https://doi.org/10.1029/2007GL032998

Sagawa, E., Immel, T. J., Frey, H. U., & Mende, S. B. (2005). Longitudinal structure of the equatorial anomaly in the nighttime ionosphere observed by IMAGE/FUV. *Journal of Geophysical Research*, *110*, A11302. https://doi.org/10.1029/2004JA010848

Titheridge, J. E. (1995). Winds in the ionosphere-a review. *Journal of Atmospheric and Terrestrial Physics*, *57*(14), 1681–1714. https://doi.org/10.1016/0021-9169(95)00091-F

Venkatraman, S., & Heelis, R. (2000). Interhemispheric plasma flows in the equatorial topside ionosphere. *Journal of Geophysical Research*, *105*(A8), 18,457–18,464. https://doi.org/10.1029/2000JA000012

Wan, W., Liu, L., Pi, X., Zhang, M.-L., Ning, B., Xiong, J., & Ding, F. (2008). Wavenumber-4 patterns of the total electron content over the low latitude ionosphere. *Geophysical Research Letters*, *35*, L12104. https://doi.org/10.1029/2008GL033755

West, K. H., & Heelis, R. A. (1996). Longitude variations in ion composition in the morning and evening topside equatorial ionosphere near solar minimum. *Journal of Geophysical Research*, *101*(A4), 7951–7960. https://doi.org/10.1029/95JA03377